Two-photon up-conversion photoluminescence realized through spatially extended gap states in quasi-2D perovskite films

*Xixiang Zhu, Hengxing Xu, Yongtao Liu, Jia Zhang, Miaosheng Wang, Ilia Ivanov, Olga S. Ovchinnikova and Bin Hu**

X. Zhu, H. Xu, J. Zhang, M. Wang, Y. Liu, Prof. B. Hu
Department of Materials Science and Engineering
University of Tennessee
Knoxville TN 37996,
E-mail: bhu@utk.edu

X. Zhu
Key Laboratory of Luminescence and Optical Information, Ministry of Education
Beijing Jiaotong University
Beijing 100044, China

Y. Liu, Dr. I. Ivanov, Dr. O. Ovchinnikova
Center for Nanophase Materials Science and Chemical and Engineering Materials Division
Oak Ridge National Laboratory
Oak Ridge, Tennessee 37831, United States

Keywords: quasi-2D perovskites, gap states, two-photon absorption, up-conversion photoluminescence, spatially extended states

Abstract

This paper reports a new approach to generate a two-photon up-conversion photoluminescence (PL) by directly exciting the gap states with continuous-wave (CW) infrared photoexcitation in quasi-2D perovskite films [$(PEA)_2(MA)_4Pb_5Br_{16}$ with n = 5]. Specifically, a visible PL peaked at 520 nm was observed with the quadratic power dependence by exciting the gap states with CW 980 nm laser excitation, indicating a two-photon up-conversion PL occurring in quasi-2D perovskites. Decreasing the gap states by reducing the n value leads to a dramatic decrease in the up-conversion PL signal. This confirms that the gap states are indeed responsible for generating the two-photon up-conversion PL in quasi-2D perovskites. Furthermore, the two-photon up-conversion PL was found to be sensitive to an external magnetic field, indicating that the gap states are essentially formed as spatially extended states ready for multi-photon excitation. Polarization-dependent up-conversion PL studies revealed that the gap states experience the orbit-orbit interaction through Coulomb polarization to form spatially extended states towards developing multi-photon up-conversion light emission in quasi-2D perovskites.

Quasi-2D perovskites have demonstrated interesting light-emitting[1-3], lasing[4,5] and photovoltaic[6-8] properties with superior stabilities. Essentially, quasi-2D perovskites are formed with the Ruddlesden-Poper perovskite (RPP) nanoplates separated by large organic ligands with the formula of $A_2A'_{n-1}M_nX_{3n+1}$.[9-12] Such 2D perovskites can demonstrate remarkable tunability on optical properties via controlling morphological structures by selecting different functional A/A' molecules.[13-15] Through down-conversion excitation, 2D perovskites have shown efficient light emission in spontaneous[16,17] and stimulated[18,19] regimes. Recently, amplified spontaneous emission (ASE) has been reported in 2D perovskites [$(NMA)_2(FA)Pb_2Br_7$ and $(NMA)_2(FA)Pb_2Br_1I_6$] with stoichiometrically tunable from visible to the near-infrared spectral range (530–810 nm) with the gain coefficient as high as > 300 cm^{-1} under pulse laser excitation.[20] On the other hand, it has been found that the edge states can be formed in 2D perovskites with light-emitting properties below the bandgap.[21] The discovery of edge states triggers a fundamental question of whether the gap states can be introduced as a new approach to develop multi-photon up-conversion light emission in RPP 2D perovskites. We should note that an up-conversion ASE was indeed observed at 720 nm in inorganic 2D perovskite ($CsPbI_3$) under the infrared pulse laser excitation of 1200 nm.[22] In this work, we explore CW infrared excitation-induced up-conversion PL in quasi-2D perovskite [$(PEA)_2(MA)_4Pb_5Br_{16}$ (n=5)] films by directly exciting gap states. The n values were selected at n = 1, n = 2, n =3, n = 4, and n = 5 to adjust the density of gap states. Here, we found that an up-conversion PL can be observed in 2D perovskite [$(PEA)_2(MA)_4Pb_5Br_{16}$ (n=5)]films under CW 980 nm excitation when broad infrared absorption is occurred between 800 nm and 1500 nm. To further understand the up-conversion PL under CW infrared excitation, magnetic field effects of PL (namely magneto-PL) were used to identify whether the gap states function as spatially extended states to generate multi-photon absorption in quasi-2D perovskite films. Furthermore, circular polarization-dependent PL was used to explore the effects of orbit-orbit interaction on up-conversion PL under CW 980 nm excitation. Technically, up-conversion

photoluminescence can find promising applications in infrared sensing, biological imaging, photocatalysis.[23-25]

Figure 1a shows the optical absorption and PL spectra for the quasi-2D perovskite $(PEA)_2(MA)_4Pb_5Br_{16}$ (n=5) films. The absorption spectrum illustrates a broad band in near-infrared spectrum ranging from 800 nm to 1500 nm, indicating the existence of gap states in the quasi-2D perovskite ($(PEA)_2(MA)_4Pb_5Br_{16}$) films. Interestingly, when the CW 980 nm laser of 750 mW/cm^2 is used to directly excite the gap states, a visible light emission becomes appeared with the spectral peak wavelength of 520 nm (Figure 1b). This observation provides the direct evidence that the gap states can be used to generate the up-conversion PL under CW infrared 980 nm laser excitation in the quasi-2D perovskite films. Figure 1c presents up-conversion PL intensity as a function of CW infrared 980 nm laser intensity. The power dependence with the slope of 1.7 indicates that the up-conversion PL is essentially a two-photon process enabled by directly exciting gap states in the quasi-2D perovskite ($(PEA)_2(MA)_4Pb_5Br_{16}$, n = 5) films.

Now we further investigate the two-photon up-conversion PL in the relationship with gap states in RPP nanoplates by adjusting n value. **Figure 2a** shows the X-ray diffraction (XRD) to confirm the crystalline structures of quasi-2D perovskite films of $(PEA)_2(MA)_{n-1}Pb_nBr_{3n+1}$ with different n values. Here, we can see that decreasing the n value leads to a reduction on the infrared absorption between 800 nm and 1500 nm in the RPP nanoplates, indicating the decrease of gap states (Figure 2b). Simultaneously, the two-photon up-conversion PL largely decreases when decreasing the gap states through reducing the n value under CW 980 nm laser excitation (Figure 2c). The up-conversion PL signal becomes negligible when the n < 3. This confirms that the gap states are indeed serving as the new approach to generate two-photon up-conversion PL in RPP nanoplates. It has been reported that a lower-energy photoexcitation below bandgap can generate a high-energy PL above bandgap in 2D perovskite ($(C_6H_5C_2H_5NH_3)_2PbI_4$), leading to a photoinduced cooling effect.[26] Essentially, this is an one-

photon up-conversion PL through electron-phonon coupling with the assistance from thermal energy. On the other hand, the edge states have been observed from the light emission with the energy lower than the bandgap in quasi-2D perovskites ($(BA)_2(MA)_{n-1}Pb_nI_{3n+1}$).[21] Here, we observed a broad infrared absorption, shown as gap states to generate two-photon up-conversion PL, in our quasi-2D perovskite ($(PEA)_2(MA)_4Pb_5Br_{16}$) films. Although the origin of gap states demands further investigations, we hypothesize that the gap states are formed from structural deformation on RPP nanoplates in quasi-2D perovskite films based on the relationship between n value and infrared absorption. This can be understood by the assumption that increasing the n value can decrease the potential barriers to form structural deformation during the crystallization of RPP nanoplates, leading to an increase on gap states. This hypothesis suggests that the gap states, responsible for two-photon up-conversion PL, are essentially formed within lattice structures coupled with the band structures in quasi-2D perovskites.

To further understand the gap states responsible for two-photon up-conversion PL, we compared the quasi-2D perovskite ($(PEA)_2(MA)_4Pb_5Br_{16}$) films prepared without and with anti-solvent processing. The crystalline structures of quasi-2D ($(PEA)_2(MA)_4Pb_5Br_{16}$) perovskite films prepared without anti-solvent processing are shown in XRD (Figure S3, Supporting Information). Here, we found that the up-conversion PL became undetectable in the quasi-2D ($(PEA)_2(MA)_4Pb_5Br_{16}$) perovskite films prepared without anti-solvent processing. Particularly, without anti-solvent processing the quasi-2D perovskite films show dissimilar PL spectra measured from the bottom and top surfaces (**Figure 3a**), indicating an in-sufficient energy transfer between different-n-value nanoplates. On contrast, with anti-solvent processing the quasi-2D perovskite films exhibit similar PL spectra measured from bottom and top surfaces, showing a sufficient energy transfer. Here, the quasi-2D perovskite films prepared without and with anti-solvent processing show short and long PL lifetimes (Figure 3d), confirming the high and low densities of defects, respectively. Obviously, the high density of defects disables two-

photon up-conversion PL in quasi-2D perovskite films under CW 980 nm laser excitation. Moreover, without anti-solvent processing the quasi-2D perovskite films demonstrate negligible infrared absorption (Figure 3c), indicating the absence of gap states in quasi-2D ($(PEA)_2(MA)_4Pb_5Br_{16}$) perovskite films. Clearly, the gap states cannot be formed in quasi-2D perovskite films with high density of defects, disabling two-photon up-conversion PL under CW 980 nm excitation.

Quasi-2D perovskites are normally formed with different-n-value nanoplates.[27-29] The energy transfer between different-n-value nanoplates is the key issue to determine the optical properties in 2D perovskites.[2,11,28,30] In general, the RPP nanoplates with different n values can be arranged with non-uniform and uniform dispersions in quasi-2D perovskite films. In the non-uniform dispersion the RPP nanoplates are arranged from lower n value with higher bandgap to larger n value with smaller bandgap between the bottom and top surfaces in quasi-2D perovskite films. This allows the energy transfer occurring from the bottom surface with lower-n-value nanoplates to the top surface with higher-n-value plates, but suppresses the energy transfer from the top to the bottom surface. The non-uniform dispersion of RPP nanoplates can be reflected by dissimilar PL spectra with different spectral peaks when exciting the bottom and top surfaces. In uniform dispersion, the RPP nanoplates are homogeneously mixed between different n values in quasi-2D perovskite films. This enables the energy transfer bi-directionally between the bottom and top surfaces in quasi-2D perovskite films. The uniform dispersion of RPP nanoplates can be shown as very similar PL spectra when exciting the bottom and top surfaces. Here, we can see that our quasi-2D perovskite ($(PEA)_2(MA)_4Pb_5Br_{16}$) films demonstrate similar PL spectra with the same peak wavelength at 521 nm while exciting the bottom and top surfaces (Figure 3b). Interestingly, there is no detectable light emission observed at short wavelengths from lower-n-value nanoplates in our quasi-2D perovskite films (Figure S1, Supporting Information). This indicates that the uniform dispersion of RPP nanoplates lead to an efficient energy transfer from lower-n-value nanoplates to large-n-value

nanoplates in our quasi-2D perovskite ($(PEA)_2(MA)_4Pb_5Br_{16}$) films. To further understand the energy transfer occurring in excited states, the quasi-2D perovskite LEDs were fabricated with the device architecture of ITO/PEDOT/$(PEA)_2(MA)_4Pb_5Br_{16}$/B-phen/LiF/Ag (Figure S2, Supporting Information). The electroluminescence (EL) spectrum shows only one peak at 521 nm from the nanoplates with n = 5, identical to the PL peak, without any detectable emission from the lower-n-value nanoplates. Because the EL is governed by carrier transfer between different nanoplates,[2,30] the similarity between PL and EL spectra indicates that the efficient energy transfer in excited states is dominated by carrier transport from lower-n-value nanoplates to larger-n-value nanoplates in our quasi-2D perovskite ($(PEA)_2(MA)_4Pb_5Br_{16}$) films where different-n-value nanoplates are uniformly dispersed under anti-solvent processing.

Now we further discuss the characteristics of gap states responsible for inducing two-photon up-conversion light emission in quasi-2D perovskite ($(PEA)_2(MA)_4Pb_5Br_{16}$) films by using magneto-PL. Our early studies have shown that magneto-PL can be observed when spatially extended states are formed with the characteristics similar to charge-transfer states and polaron pairs.[31-33] This is because spatially extended states have weaker exchange interaction, allowing spin mixing to occur between different states and leading to a magneto-PL. On contrast, the localized excited states such as Frenkel excitons do not exhibit any detectable magneto-PL due to strong exchange interaction which does not allow spin mixing to occur between different states.[31,32] Therefore, magneto-PL can be used as an *in-situ* method to elucidate the characteristics of gap states responsible for two-photon up-conversion PL in quasi-2D perovskites. **Figure 4a** shows both up-conversion and down-conversion PL intensities measured with and without the constant magnetic field of 300 mT in our quasi-2D perovskite ($(PEA)_2(MA)_4Pb_5Br_{16}$) films. We can see that applying the magnetic field can appreciably increase the up-conversion PL intensity under CW 980 nm laser excitation while the down-conversion PL does not show any detectable magnetic field dependence under CW 488 nm laser excitation. This provides an evidence that the gap states are essentially functioning as spatially

extended states in RPP nanoplates to enhance multi-photon absorption towards generating up-conversion light emission. To further understand the characteristics of gap states, the two-photon up-conversion PL was measured with linearly and circularly polarized CW 980 nm laser excitations at the same intensity. Here, a circularly polarized excitation excites the orbitals with same-directional magnetic dipoles between excited states while a linearly polarized excitation excites the orbitals with opposite-directional magnetic dipoles between excited states. When the orbit-orbit interaction occurs, the same-directional and opposite-directional magnetic dipoles give rise to stronger and weaker orbital-magnetic dipole moments to generate more and less spin mixing from bright states to dark states, respectively. Essentially, switching the photoexcitation between linear and circular polarizations causes a change on PL intensity, leading to a ΔPL if the orbit-orbit interaction occurs.[34,35] Therefore, monitoring ΔPL upon switching photoexcitation between linear and circular polarizations can reflect whether the gap states, functioning as spatially extended states, are involved in orbit-orbit interaction. **Figure 5** shows the PL intensity monitored at 520 nm during switching the photoexcitation between linear and circular polarizations under CW 980 nm laser excitation. We can see that the up-conversion PL exhibits a polarization dependence of photoexcitation, leading to a clear ΔPL. Clearly, the observed ΔPL reveals that the gap states experience orbit-orbit interaction, providing the precondition to form spatially extended states towards developing two-photon up-conversion PL in quasi-2D perovskites. On contrast, the down-conversion PL intensity shows a negligible change during switching the CW 480 nm excitation between linear and circular polarizations. This indicates that the excited states responsible for down-conversion are less involved in orbit-orbit interaction as compared to spatially extended gap states in quasi-2D perovskites. Furthermore, we should point out that orbit-orbit interaction consists of magnetic and Coulombic components. The magnetic component results from the interaction between orbital-magnetic dipoles. The Coulombic component is essentially the orbital-polarization

interaction. When the magnetic component dominates the orbit-orbit interaction, the linear photoexcitation generates a stronger PL intensity as compared to circular photoexcitation. This is because circular photoexcitation creates same-directional magnetic dipoles between optically excited orbitals and consequently causes a stronger spin mixing from bright to dark states through spin-orbital coupling effects, generating a -ΔPL by switching the photoexcitation from linear to circular polarization.[36] When the Coulombic component dominates the orbit-orbit interaction, the circular photoexcitation generates a stronger PL intensity as compared to linear photoexcitation. This is because linear photoexcitation initiates the polarization interaction between optically excited orbitals and consequently produces a stronger spin mixing from bright to dark states through spin-orbital coupling effects, leading to a positive +ΔPL by switching photoexcitation from linear to circular polarization.[36] Based on this analysis, we can see from the observed +ΔPL that the gap states are formed as spatially extended states through orbit-orbit interaction dominated by Coulombic polarization to generate two-photon up-conversion light emission in quasi-2D perovskite ($(PEA)_2(MA)_4Pb_5Br_{16}$) films (**Figure 6**).

In summary, we found that optically exciting the gap states can lead to an infrared-to-visible up-conversion PL in quasi-2D perovskite ($(PEA)_2(MA)_4Pb_5Br_{16}$) films with uniform dispersion of nanoplates at room temperature under CW infrared 980 nm laser excitation. The quadratic dependence between excitation and emission intensities indicates that the up-conversion PL essentially results from a two-photon excitation process. When the gap states are decreased by reducing the n value in the RPP nanoplates, the two-photon up-conversion PL becomes negligible in quasi-2D perovskite films when the $n < 3$. This confirms that the gap states are indeed responsible for generating the two-photon up-conversion light emission. More importantly, the two-photon up-conversion PL is sensitive to the magnetic field, leading to a magneto-PL upon optically exciting the gap states by using CW infrared 980 nm laser beam. This observation indicates that the gap states are essentially formed as spatially extended states

in larger-n-value nanoplates. Furthermore, polarization-dependent PL studies show that the gap states experience orbit-orbit interaction dominated by orbital polarization to develop into spatially extended states. Clearly, the gap states functioning as spatially extended states allow the two-photon absorption to generate an up-conversion light emission in quasi-2D perovskite films.

Experimental Section

Materials and Methods: Quasi-2D perovskites [$(PEBr)_2(MA)_{n-1}Pb_nBr_{3n+1}$] were prepared by dissolving stoichiometric quantities of lead bromide ($PbBr_2$), methylammonium bromide (MABr), and phenylethylammonium bromide (PEABr) with the ratios of 0.6:0:1.2, 0.6:0.3:0.6, 0.6:0.4:0.4, 0.6:0.45:0.3 and 0.6:0.48:0.24 (mol:mol:mol) for n=1 to 5 in the dimethyl sulfoxide (DMSO), respectively. All of the solutions were stirring at 60 °C for 12 hours and then spin-coated onto quartz substrates by using two steps: 500 rpm for 6 seconds and 3000 rpm for 60 seconds. During the second spin-coating step, 200 μl toluene was dripped on the perovskite films for 30 seconds. All spin-cast films were thermally annealed at 90 °C for 10 minutes. The 2D perovskite LEDs were fabricated by spin-casting the $(PEA)_2(MA)_4Pb_5Br_{16}$ films (300 nm thickness) on ITO/PEDOT substrates, followed by thermally evaporating 30 nm thick B-phen, 1 nm LiF, and 80 nm thick Ag top electrode to form the device architecture of ITO/PEDOT/$(PEA)_2(MA)_4Pb_5Br_{16}$/B-phen/LiF/Ag. The magneto-PL were performed by recording PL peak intensity with and without the constant magnetic field of 300 mT. The magnitude of magneto-PL is defined as $\frac{I_{(B)}-I_{(0)}}{I_{(0)}}$, where the $I_{(B)}$ and $I_{(0)}$ are PL intensities with and without magnetic field, respectively. The ΔPL was measured upon switching the photoexcitation between linear and circular polarizations at same intensity by rotating quarter

wave plate with 0° and 45° relative to a linear polarizer. The ΔPL was calculated by $\frac{I_{(L)}-I_{(C)}}{I_{(L)}}$, where $I_{(L)}$ and $I_{(C)}$ are defined as PL intensities generated by linear and circular photoexcitations.

Supporting Information

Supporting Information is available from the Wiley Online Library or from the author.

Acknowledgements

This research was supported by Air Force Office of Scientific Research (AFOSR) (FA 9550-15-1-0064, FA2386-15-1-410) and National Science Foundation (NSF-1911659). This research was partially conducted at the Center for Nanophase Materials Sciences based on user projects (CNMS2012-106, CNMS2012-107, CNMS-2012-108, CNMS-2019-057), which is sponsored by Oak Ridge National Laboratory by the Division of Scientific User Facilities, U.S. Department of Energy. The author X. Zhu acknowledges the project support from National Natural Science Foundation of China (Grant no. 61475051, 61634001), Significant National Program (2014CB643506, 2013CB922104) and Beijing Jiaotong University (2017JBZ105).

Received: ((will be filled in by the editorial staff))
Revised: ((will be filled in by the editorial staff))
Published online: ((will be filled in by the editorial staff))

References

[1] J. Byun, H. Cho, C. Wolf, M. Jang, A. Sadhanala, R. H. Friend, H. Yang, T. W. Lee, *Adv. Mater.* **2016**, *28*, 7515.

[2] M. Yuan, L. N. Quan, R. Comin, G. Walters, R. Sabatini, O. Voznyy, S. Hoogland, Y. Zhao, E. M. Beauregard, P. Kanjanaboos, *Nat. Nanotechnol.* **2016**, *11*, 872.

[3] M. Ban, Y. Zou, J. P. Rivett, Y. Yang, T. H. Thomas, Y. Tan, T. Song, X. Gao, D. Credington, F. Deschler, *Nat. Commun.* **2018**, *9*, 3892.

[4] M. Li, Q. Wei, S. K. Muduli, N. Yantara, Q. Xu, N. Mathews, S. G. Mhaisalkar, G. Xing, T. C. Sum, *Adv. Mater.* **2018**, *30*, 1707235

[5] C. M. Raghavan, T.-P. Chen, S.-S. Li, W.-L. Chen, C.-Y. Lo, Y.-M. Liao, G. Haider, C.-C. Lin, C.-C. Chen, R. Sankar, *Nano Lett.* **2018**, *18*, 3221.

[6] B. E. Cohen, M. Wierzbowska, L. Etgar, *Adv. Funct. Mater.* **2017**, *27*, 1604733.

[7] G. Grancini, C. Roldán-Carmona, I. Zimmermann, E. Mosconi, X. Lee, D. Martineau, S. Narbey, F. Oswald, F. De Angelis, M. Graetzel, *Nat. Commun.* **2017**, *8*, 15684.

[8] L. N. Quan, M. Yuan, R. Comin, O. Voznyy, E. M. Beauregard, S. Hoogland, A. Buin, A. R. Kirmani, K. Zhao, A. Amassian, *J. Am. Chem. Soc.* **2016**, *138*, 2649.

[9] S. Ruddlesden, P. Popper, *Acta Crystallogr.* **1957**, *10*, 538.

[10] S. Ruddlesden, P. Popper, *Acta Crystallogr.* **1958**, *11*, 54.

[11] N. Wang, L. Cheng, R. Ge, S. Zhang, Y. Miao, W. Zou, C. Yi, Y. Sun, Y. Cao, R. Yang, *Nat. Photonics* **2016**, *10*, 699.

[12] R. Yang, R. Li, Y. Cao, Y. Wei, Y. Miao, W. L. Tan, X. Jiao, H. Chen, L. Zhang, Q. Chen, *Adv. Mater.* **2018**, *30*, 1804771.

[13] Y. H. Kim, J. S. Kim, T. W. Lee, *Adv. Mater.* **2018**, 1804595.

[14] X. Yang, X. Zhang, J. Deng, Z. Chu, Q. Jiang, J. Meng, P. Wang, L. Zhang, Z. Yin, J. You, *Nat. Commun.* **2018**, *9*, 570.

[15] X. Xiao, J. Dai, Y. Fang, J. Zhao, X. Zheng, S. Tang, P. N. Rudd, X. C. Zeng, J. Huang, *ACS Energy Lett.* **2018**, *3*, 684.

[16] L. N. Quan, Y. Zhao, F. P. García de Arquer, R. Sabatini, G. Walters, O. Voznyy, R. Comin, Y. Li, J. Z. Fan, H. Tan, *Nano Lett.* **2017**, *17*, 3701.

[17] Z. Yuan, Y. Shu, Y. Xin, B. Ma, *Chem. Commun.* **2016**, *52*, 3887.

[18] W. Zhang, L. Peng, J. Liu, A. Tang, J. S. Hu, J. Yao, Y. S. Zhao, *Adv. Mater.* **2016**, *28*, 4040.

[19] H. Zhang, Q. Liao, Y. Wu, Z. Zhang, Q. Gao, P. Liu, M. Li, J. Yao, H. Fu, *Adv. Mater.* **2018**, *30*, 1706186.

[20] M. Li, Q. Gao, P. Liu, Q. Liao, H. Zhang, J. Yao, W. Hu, Y. Wu, H. Fu, *Adv. Funct. Mater.* **2018**, *28*, 1707006.

[21] J.-C. Blancon, H. Tsai, W. Nie, C. C. Stoumpos, L. Pedesseau, C. Katan, M. Kepenekian, C. M. M. Soe, K. Appavoo, M. Y. Sfeir, *Science* **2017**, *355*, 1288.

[22] Z. Zheng, X. Wang, Y. Shen, Z. Luo, L. Li, L. Gan, Y. Ma, H. Li, A. Pan, T. Zhai, *Adv. Opt. Mater.* **2018**, *6*, 1800879.

[23] F. Wang, D. Banerjee, Y. Liu, X. Chen, X. Liu, *Analyst* **2010**, *135*, 1839.

[24] J. Zhou, Q. Liu, W. Feng, Y. Sun, F. Li, *Chem. Rev.* **2014**, *115*, 395.

[25] R. Deng, F. Qin, R. Chen, W. Huang, M. Hong, X. Liu, *Nat. Nanotechnol.* 2015, *10*, 237.

[26] S.-T. Ha, C. Shen, J. Zhang, Q. Xiong, *Nat. Photonics* **2016**, *10*, 115.

[27] G. Xing, B. Wu, X. Wu, M. Li, B. Du, Q. Wei, J. Guo, E. K. Yeow, T. C. Sum, W. Huang, *Nat. Commun.* **2017**, *8*, 14558.

[28] Q. Shang, Y. Wang, Y. Zhong, Y. Mi, L. Qin, Y. Zhao, X. Qiu, X. Liu, Q. Zhang, *J. Phys. Chem. Lett.* **2017**, *8*, 4431.

[29] L. Pedesseau, D. Sapori, B. Traore, R. Robles, H.-H. Fang, M. A. Loi, H. Tsai, W. Nie, J.-C. Blancon, A. Neukirch, *ACS Nano* **2016**, *10*, 9776.

[30] P. Chen, Y. Meng, M. Ahmadi, Q. Peng, C. Gao, L. Xu, M. Shao, Z. Xiong, B. Hu, *Nano Energy* **2018**, *50*, 615.

[31] L. He, M. Li, A. Urbas, B. Hu, *Phys. Rev. B* **2014**, *89*, 155304.

[32] B. Hu, L. Yan, M. Shao, *Adv. Mater.* **2009**, *21*, 1500.

[33] Y. C. Hsiao, T. Wu, M. Li, B. Hu, *Adv. Mater.* **2015**, *27*, 2899.

[34] J. Zhang, T. Wu, J. Duan, M. Ahmadi, F. Jiang, Y. Zhou, B. Hu, *Nano Energy* **2017**, *38*, 297.

[35] W. Qin, H. Xu, B. Hu, *ACS Photonics* **2017**,*4*, 2821.

[36] H. Xu, M. Wang, Z. Yu, K. Wang, B. Hu, *Adv. Phys*. **2019**, *68*, 49

Figures

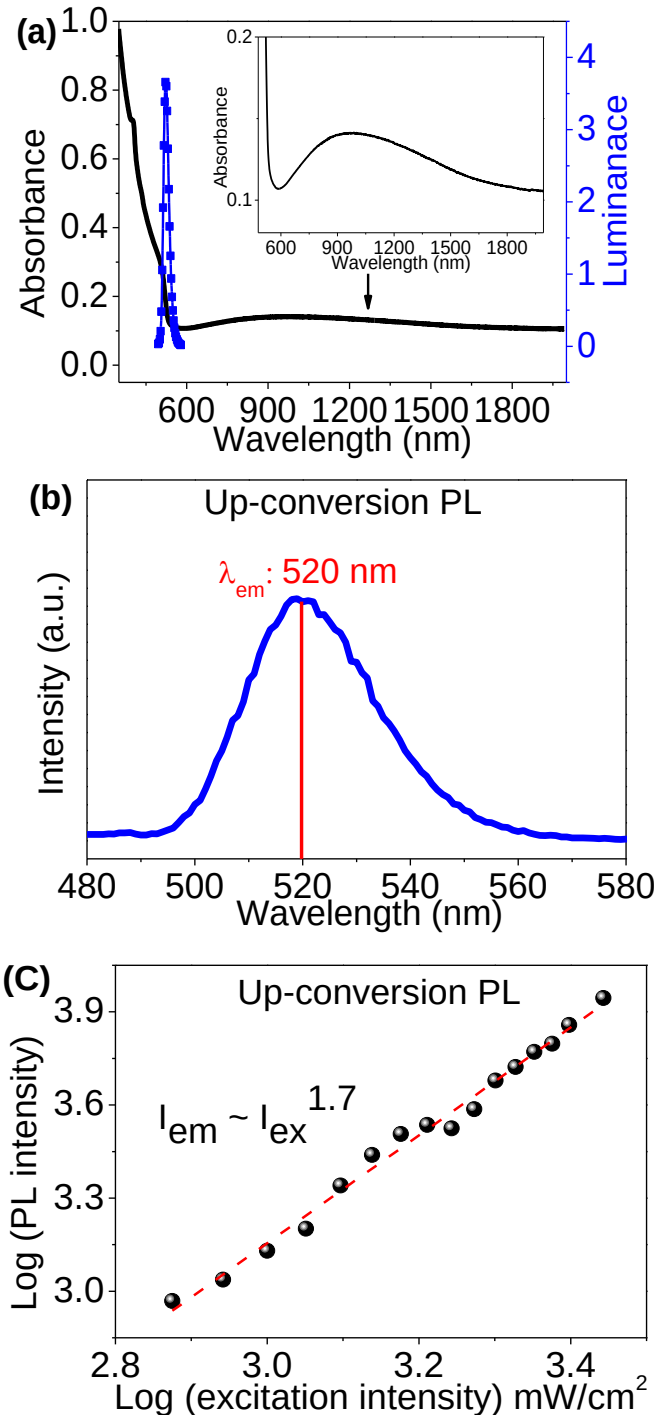

Figure 1. Absorption and down-conversion PL characteristics for 2D perovskite $(PEA)_2(MA)_4Pb_5Br_{16}$ films. (a) Absorption and PL spectra. (b) Up-conversion PL spectrum under CW 980 nm laser excitation (2500 mW/cm^2). (c) Emission-excitation intensity dependence under up-conversion condition.

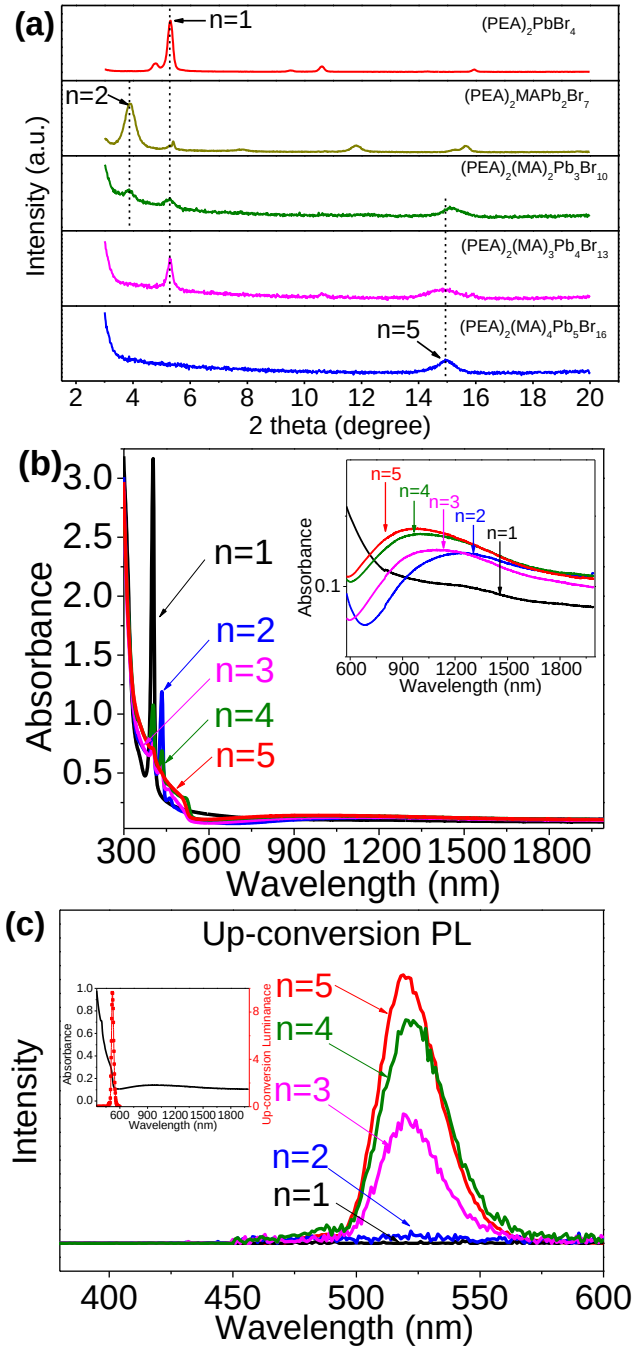

Figure 2. Gap states and up-conversion PL for RPP nanoplates with different n values in uniform dispersion quasi-2D perovskite [$(PEA)_2(MA)_{n-1}Pb_nBr_{3n+1}$] films. (a) XRD patterns. (b) Absorption spectra measured from 300 nm to 200 nm for quais-2D perovskite films with different n values. Inset: infrared absorption spectra plotted from 600 nm to 2000 nm. (c) Up-conversion PL spectra under CW 980 nm laser excitation (2500 mW/cm^2). Inset: normalized up-conversion and absorption spectra.

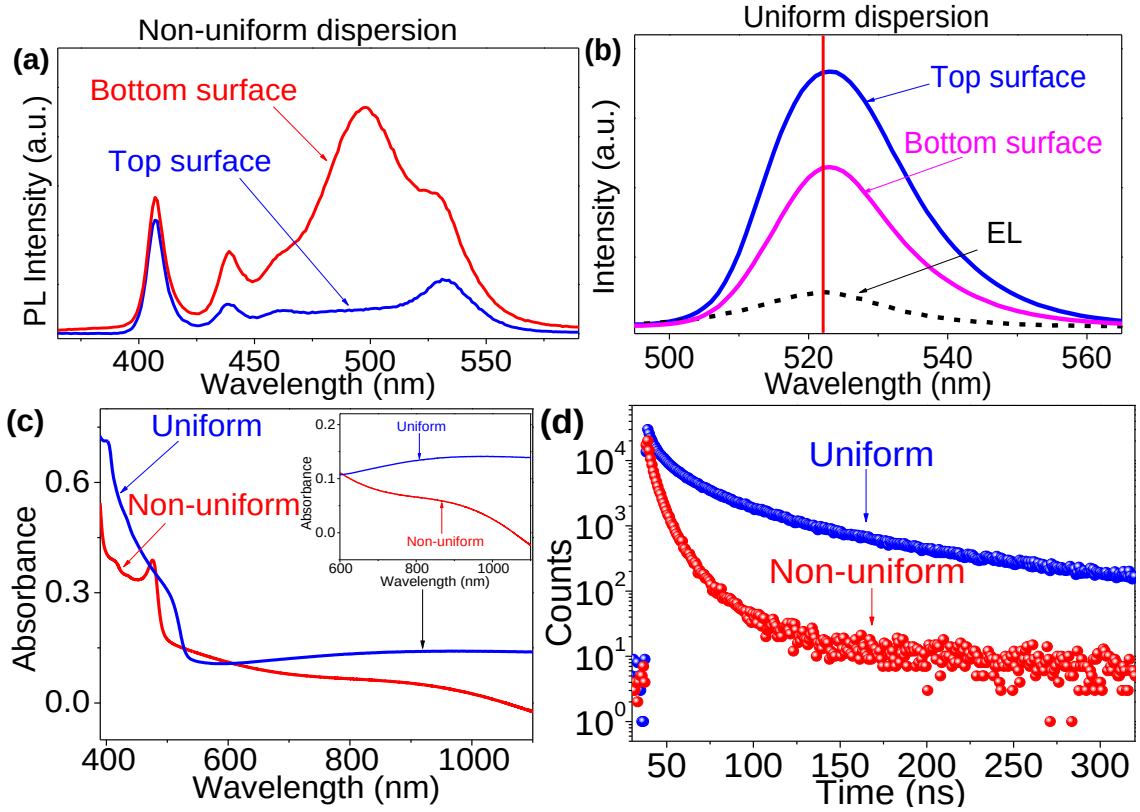

Figure 3. Spectral characteristics for quasi-2D perovskite $(PEA)_2(MA)_4Pb_5Br_{16}$ films with uniform and non-uniform dispersions of nanoplates. (a) PL spectra for non-uniform dispersion of RPP nanoplates (optically exciting top and bottom surfaces with 325 nm excitation). (b) PL spectra for uniform dispersion of RPP nanoplates (optically exciting top and bottom surfaces with 488 nm CW laser excitation of 14 mW/cm^2). The dashed spectrum is shown as EL from ITO/PEDOT/$(PEA)_2(MA)_4Pb_5Br_{16}$/B-phen/LiF/Ag device. (c) Absorption spectra for non-uniform and uniform dispersions of RPP nanoplates. Inset: Infrared absorption for uniform and non-uniform dispersions. (d) Time-resolved photoluminescence (TRPL) spectra for non-uniform and uniform dispersions of RPP nanoplates.

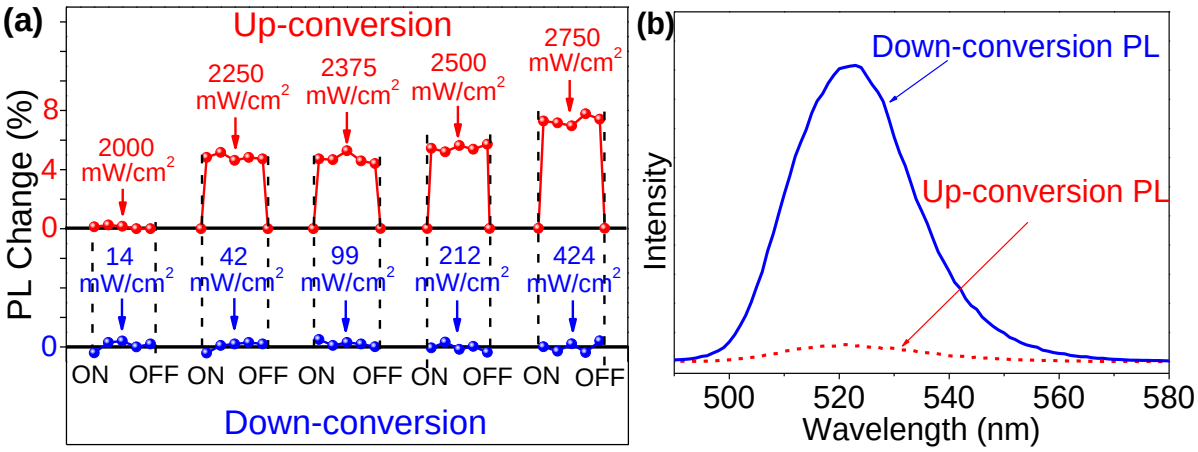

Figure 4. Magneto-PL measured under up-conversion and down-conversion conditions in quasi-2D perovskite $(PEA)_2(MA)_4Pb_5Br_{16}$ films. The magnetic field was set at 300 mT. (a) Magneto-PL measured under up-conversion (red color) and down-conversion (blue color) conditions excited by CW 980 nm and 488 nm lasers at different intensities. (b) Up-conversion and down-conversion light emission used for magneto-PL measurements.

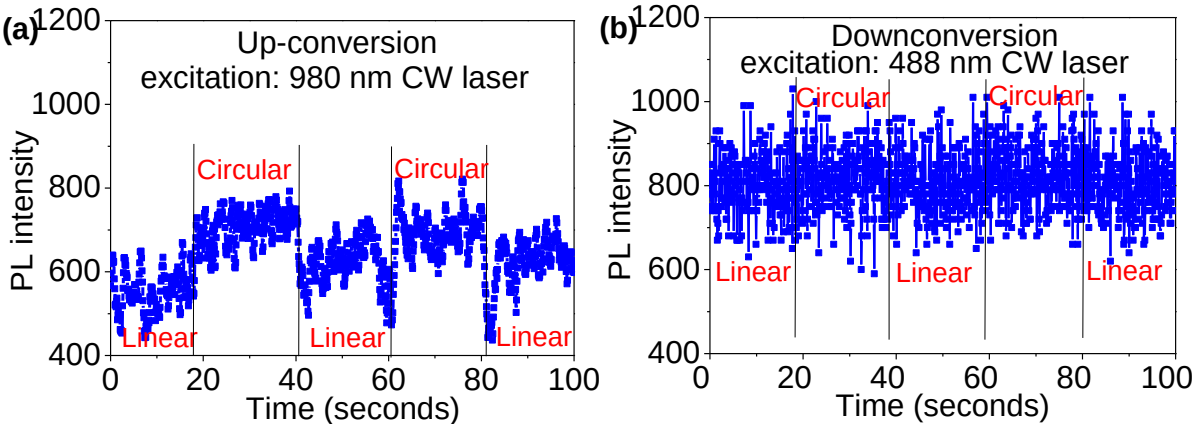

Figure 5. Up-conversion and down-conversion PL intensities under linear and circular photoexcitations. (a) Up-conversion operated by linearly and circularly polarized 980 nm CW laser excitations. (b) Down-conversion operated by linearly and circularly polarized 488 nm CW laser excitations.

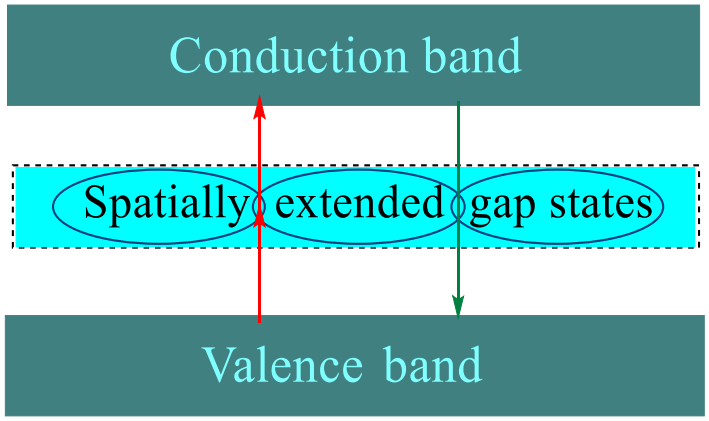

Figure 6. Schematic diagram to show gap states, functioning as spatially extended states through orbit-orbit interaction, to generate two-photon up-conversion excitation.